J Sol-Gel Sci Technol (2017) 82:551–562
DOI 10.1007/s10971-017-4309-z

ORIGINAL PAPER: SOL-GEL AND HYBRID MATERIALS FOR OPTICAL, PHOTONIC AND OPTOELECTRONIC APPLICATIONS

Composite rods based on nanoscale porous silicon in sol–gel silica and ormosil matrices for light-emitting applications

M. Naziruddin Khan[1] · Ali Aldalbahi[1] · A. S. Al Dwayyan[2]

Received: 12 August 2016 / Accepted: 15 January 2017 / Published online: 28 January 2017

Abstract In this paper, we report a new approach for fabrication of porous silicon (PSi) composites sol–gel-based matrix rods. PSi colloidal solutions were directly encapsulated in two types of sols prepared by the sol–gel process. The property of nanocomposite silica and ormosil matrix was investigated by optical techniques. Absorption and its band gap of PSi in silica and ormosils are influenced by matrix environment. Emission properties of PSi are affected by the surrounding matrix and temperature. The morphology of nanocomposites was characterized by scanning electron microscopy, indicating the dissimilar surface structure of the PSi in the matrix. The PSi particles in the matrices are well distributed with more or less 5–8 nm size as confirmed by transmission electron microscopy. Crack-free PSi composite silica and ormosil-based rods were successfully developed. The cutting and polishing of the surface of rods was performed. Subsequently, spontaneous emission of the rods was examined using a high pico second 355 nm laser source. The enhanced emission from the nanocomposite ormosils is remarkable and more prominent than the nanocomposite silica rod. Such typical spontaneous emission from nanocomposite rods indicates that it may be possible to improve if highly dense PSi colloidal solution is used. The present results are of benefit in further understanding more about the photoluminescence mechanism of PSi in the matrices.

Graphical Abstract

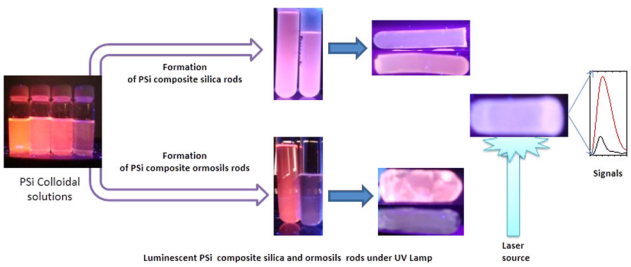

Keywords Porous silicon, sol–gel matrices · Absorption and Photoluminescence spectra · Spontaneous emission · Scanning electron microscope · Transmission electron microscopy · 355 nm pico second laser source

1 Introduction

Silicon-based nanocrystalline materials have been of extensive interest because of their promising nature for new photoelectronic and informational applications. Earlier, it had been considered an unsuitable material for optoelectronics since it emits hardly any useful light due to the indirect band gap nature [1]. The first discovery of bright emission from porous silicon (PSi) and nanocrystals silicon (ncs-Si) had changed the idea [2] for many applications. Since then, the concern of constructing Si-based optoelectronic devices such as integrated circuits [3, 4] has greatly generated especially in the preparation and characterization

✉ M. Naziruddin Khan
mnkhan_phy@yahoo.com

[1] King Abdullah Institute for Nanotechnology, King Saud University, Riyadh 11451, Saudi Arabia

[2] Physics and Astronomy Department, College of Science, KSU, Riyadh 11451, Saudi Arabia

of light-emitting silicon nanoparticles. Enormous studies on Si nanoparticles have been performed due to their luminescence depending on sizes and multi-colors, which have exciting potential applications as fluorescent tags for biological imaging [5, 6] and for bio-analysis including quantum dots [7].

However, significant studies have been carried out on the silicon porous nanoparticles mainly aimed at solar application due to its potential to increase efficiency [8]. Moreover, silicon nanostructured materials have appeared in the literature to be promising for energy storage and conversion devices [9, 10]. Nonetheless, the use of PSi/ncs-Si as an active medium for light-emitting devices (LEDs or injection laser) remains an open topic for basic research, even though PSi/ncs-Si have potential for various applications in waveguides and photodetectors [11]. The tough and challenging task is to realize the optical gain or lasing in silicon for optoelectronic circuits, because the silicon-based light source is a key component from application points of view. In this respect, a few studies have been carried out exclusively on the silicon nanocrystals (Si-NC) in an insulator matrix, usually SiO_2 films, because of their optical properties [12, 13] and the role of interface between the Si-NC and the oxide matrix [14–16], which is believed to be an important parameter for controlling the optoelectronic properties. The techniques used to produce an Si-NC structure are the implementation of silicon ions into an SiO_2 matrix by thermal annealing [17, 18], sputtering of Si rich oxides [19], or reactive evaporation of Si-rich oxides [20]. But silicon nanoparticles with strong light emission in a host matrix prepared at low temperature with a smallest band gap is highly desirable for stabilizing and controlling emission of PSi. In addition, the demonstration of PSi /ncs-Si within the low temperature-based matrices of such sol–gels is easily manageable, which helps to fabricate the samples with high densities of nanoparticles for optoelectronics purposes.

Recently, a great variety of Si nanostructures have been studied to maintain and stabilize its photoluminescence (PL) by directly encapsulating within the sol–gel-derived fine powder [21], sol–gel-derived films [22], composite blocks of silica matrix [23], silica aerogel pellet composites [24], blocks of aerogel [25], and in aerogel films [26]. Despite few efforts, there is not yet full understanding of the optical stability of PSi/ncs-Si composites' sol–gel-derived matrices that may lead to Si as a material for light amplification. In fact, limited work on the direct encapsulation of PSi/nc-Si in different composition-based matrices such as sol–gel matrix or organically modified silicates (ormosils) was performed previously. Our group reported a series of studies on PL and the structural properties of the ncs-Si powder in sol–gel [27] and temperature's influence on the interface of ncs-Si and sol–gel hosts [28], and nanoporous silicon [29–31]. In these works, we employed the PSi or ncs-Si powder colloidal solutions in different silica matrices using different co-solvents and drying control chemical addition (DCCA) in the sol-gel process. In continuation of the above, we extend the study of PSi in sol–gel-derived ormosil-type hosts [32], which offer several advantages over pure sol–gel silica, such as being crack free, low light scattering, better mechanical properties, flexibility, and easy hand polish. The main interest of the present study is (i) to understand the effects on optical, PL emission, and structural properties of PSi in the environment of two different composition-based matrices such as silica and ormosils and (ii) finally to transform the composite silica and ormosil matrix into rod shape, which could be used to examine the characteristics of spontaneous emission (SE) under the tunable laser source.

2 Experiment and materials

2.1 Porous silicon

The electrochemical etching technique is widely used to produce porous silicon in an electrolyte solution of hydrofluoric acid (HF) and solvents by applying an electrical source [33, 34]. On the other hand, the efficient room temperature luminescence in PSi can be produced by simple chemical etching (without applying current) and was earlier reported in [35, 36]. In the present work, a simple electroless chemical etching process was employed, which is reported in detail in [29–31]. Shortly, nanoscale porous silicon was fabricated by using a highly catalyst solution of 40% HF, hexachloroplatinic (IV) acid (H_2PtCl_6), deionized water and etchant solution of methanol, HF and 30% H_2O_2 to convert crystalline Si into ultrasmall nanoparticles. In fact, HF is highly reactive with silicon oxide and H_2O_2 catalyzes the etching, which enables to produce smaller particles from the surface of silicon wafer. Also, the oxidative nature of the peroxides can produce high chemical and electronic quality samples. The single P-type boron-doped Si wafers (100, 1–10 ohm) were used and made into small rectangular pieces. The size and quantity of the rectangular pieces used were 1×4 cm and 6, respectively. The wafer pieces were ultrasonically cleaned with acetone and dried with N_2 gas. The etched wafer pieces were rinsed in isopropanol and dried slowly with N_2 gas. The pulverized wafer pieces were transferred into the solvent of interest that was used, 1,4-dioxane. The volume of dioxane solvent was taken as 20 ml. This PSi colloidal solution was exposed to an UV lamp at 365 nm in order to check luminescent light.

2.2 Sol–gel silica matrix

Silica matrix was prepared by a conventional three-step-based sol–gel process as in our previous reported work in which preparation of sols involved reacting tetraethylorthosilicate (TEOS) with different co-solvents such as ethanol, THF, dioxane, and a DCCA such as dimethylformamide (DMF), which is described in more detail elsewhere [27–30]. The role of solvent in the sol–gel preparation is considered as an important parameter especially during the drying and aging of the matrix. In addition, the mixing of a DCCA in the sol–gel process can yield good qualities in the matrix, such as monolithicity, low density, transparency, the pore size distribution, and uniformity. Further, DCCA controls the speed of hydrolysis and condensation that usually influences the dopants in sol–gel matrices [37].

Moreover, the key role of DCCA is to change the structure of the sol–gel material. For instance, DCCA (e.g., formamide, DMF, DMSO) drives the generation of large pores with narrow size distribution. The larger pore size causes the weakening of capillary forces and the stress exerted on the gel during drying is smaller. On the other hand, the mechanism of action is the binding of the DCCA to the silica surface through the formation of hydrogen bonds. This helps to remove the water molecules by halting the interaction with silanol groups on the pore walls [38].

In the present sol–gel process, the starting inorganic precursor was taken as TEOS (Aldrich, 98%), with co-solvent as dioxane solvent (WinLab, 99%) without further purification. The silica sols were prepared from hydrolysis and polycondensation of TEOS using dioxane as co-solvent, formamide as DCCA instead of DMF, nitric acid as catalyst, and distilled water. The PSi colloidal suspension dioxane was introduced into the mixture sol of molar ratio 1:1.5:0.5:1:0.01 (TEOS:dioxane:formamide:water: nitric acid, respectively). About 8 ml of PSi colloidal solution was then added to 6 ml of sol and treated ultrasonically for about 5 min to reduce the aggregate. The final PSi composite sol was transferred into quartz cuvettes and cylindrical tubes, and kept at room temperature for a week. The silica nanocomposite sols in the quartz and tube were gelled within a week at room temperature. Further, the gel samples were aged in an oven at 50–60 °C till 3 weeks to remove the liquid slowly in order to yield crack-free rod shapes. After obtaining the rods, we removed them from the polystyrene cylindrical test tube and put them in the oven for 1 day to dry up completely and become rigid.

2.3 Ormosil matrix

Ormosil matrix was prepared using SiO_2/VTEOS+MMA. In the composition, 7.43 ml of tetramethylorthosilicate (TMOS) and 10.42 ml of venyltriethylorthosilane (VTEOS) were mixed with hydrochloric acid in water (0.02 N). The molar ratio of the composition was TMOS:VTEOS: H_2O=1:1:4. The acid was use to catalyze the hydrolysis of the siloxy groups. The mixture was further stirred to achieve a single phase and formed a sol. Methyl methacrylate (MMA) monomer was mixed with the sol in equal molar amounts of the VTEOS. Benzoylperoxide (BPO) was used as initiator in an amount of 10% relative to that of MMA. The mixed solution was further stirred for about 2–3 hr to form a viscous solution. About 8 ml volume of PSi colloidal solution was then added to 6 ml of ormosil sol and stirred for about 30 min. The viscous ormosil sol was transferred into cuvettes and the cylindrical glass test tube was kept in an oven at 60 °C. The nanocomposite ormosil sols became gelled in the cuvettes and test tube after 2 days, but it took 4-5 weeks to make the rod shape. The rod was removed after the separation of ormosil surface from the glass test tube.

The concentrations of the present colloidal PSi solutions used in both matrices are unidentified since the solutions are synthesized using equal and small sizes of silicon wafer and the chemically etched wafer pieces were put in equal volume of dioxane solvent. Six milliliters of matrix sols was combined with 8 ml of PSi colloidal solution, which was originally obtained using six equal small rectangular wafer pieces in the volume of 20 ml solvent. The concentration of colloidal solutions used in the present study is assumed to be low based on their absorbance level compared to the absorbance of different solutions. In order to understand the concentration of PSi particles based on their absorption and emission property using different quantities of wafer pieces in equal volumes of different solvents, the detail results were discussed in our reported paper [31].

2.4 Measurement

A UV lamp (model XX15NF, Spectroline-USA) was used to check the luminescent light from PSi composites' sol–gel silica and ormosil solids. Microstructure images of the PSi composite samples were taken by using a field emission scanning electron microscope (JEOL, JSM-6380LA). Particle sizes were determined by depositing a drop of PSi composite sol onto a carbon-coated copper grid and taken in a HRTEM (Jeol-JEM2100F). Absorption spectra of PSi colloidal solutions, nanocomposite sol–gel silica, and ormosils were measured within the spectral range of 250–800 nm using UV-visible spectrophotometer (670 Jasco). Emission spectra of PSi colloidal solutions, nanocomposite sol–gel silica, and ormosils were recorded in the 500–700 nm spectra range using a fluorescence spectrophotometer (Lumina, Thermo UK). In both measurements, some quartz cuvettes of 10 mm path length were used to

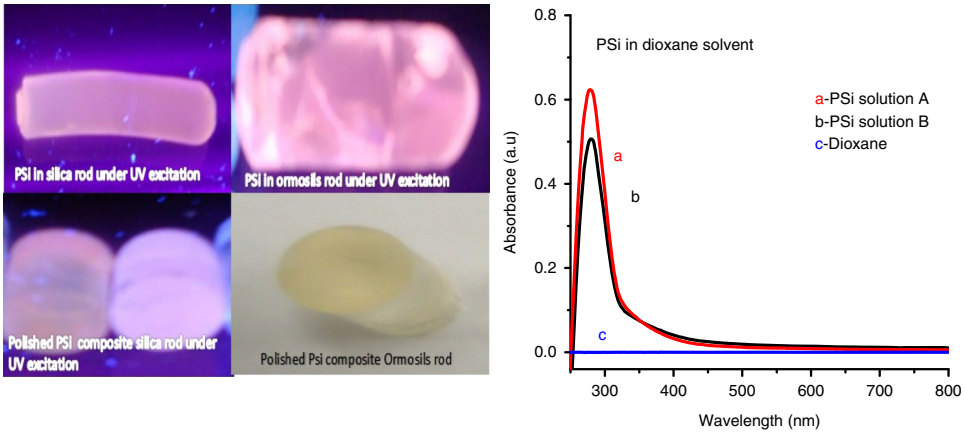

Fig. 1 **i** Luminescent PSi composite silica and ormosil rods under a UV lamp and **ii** absorption spectra of porous silicon in dioxane

measure the absorption and emission spectra of PSi colloidal solutions, nanocomposite silica, and ormosils.

Spontaneous emission spectra of PSi nanocomposite rods were examined using a 355 nm laser source of high-power pico-second tunable laser system (Loti III). The output SE from composite samples was monitored by an ICCD camera through a fiber with collimating lens.

3 Results and discussion

Direct encapsulation of colloidal PSi solutions in the sols prepared by the sol-gel process was successfully performed and did not form any sedimentation. The PSi particles are well dispersive within both the silica and ormosils sols after inclusion and even during gelification. But the size and dimension of silica-based rods are reduced during the gelling, i.e., evaporation of liquid. Sometimes cracks are formed during the gelling time if the samples are heating up directly. Cracking of samples can be controlled by aging at room temperature. After formation of rods, the remaining liquid from samples can be easily removed at a low temperature (50–60 °C) to solidify more and become rigid rods. Ormosil-based rods undergo less reduction in size and dimension during gelling because of polymerization. The PSi composite-based ormosils are found to have a slightly honey-like color when seen with the naked eye. No cracks occur with ormosil-type samples, which are more flexible unlike silica rods. A typical PSi composite silica and ormosil rod before cutting and after polishing is shown in Fig. 1i. Both composite PSi samples are seen to be luminescent under a UV lamp.

3.1 Absorption property

The absorption spectrum of two PSi colloidal solutions in the 250–500 nm region is depicted in Fig. 1ii (a, b). Usually, the signal below 250 nm in the UV region is from solvents or glass or matrices. The present signal below the 250 nm region is from dioxane solvent, as shown in Fig. 1ii (c). There is one absorption peak associated with the PSi solution. No significant change in absorption peaks of these colloidal solutions is observed. As clearly seen in Fig. 1, the observed absorption peak of both solutions is centered at 279. The optical transmission of silica and ormosil rods shown in Fig. 2i indicates the percentage of optical opaque in 200–900 nm spectra region.

The colloidal PSi dioxane solutions were directly incorporated in silica and ormosil sols to convert them to rod shape. In fact, there is no significant difference between the two solutions since PSi particles were dispersed in two equal volumes of dioxane in order to prepare nanocomposite PSi silica and ormosil matrix. Equal volumes of two colloidal solutions were incorporated into the silica and ormosil matrix. For instance, PSi solutions A and B were used in silica sols and ormosils sol, respectively. Solutions A and B were synthesized using equal rectangular sizes and number of wafer pieces (Pcs) in an equal volume of dioxane solvent. Generally, the absorption property of PSi in solution is found to be varying in those solutions synthesized using the same condition. Therefore, for the present study, two solutions were selected based on similarity to the absorption intensity in order to understand the basic optical characteristics in two different sol–gel matrices.

The absorption spectra of PSi in the sol–gel silica and ormosil matrices were investigated under the same conditions. Effect in the absorption features is observed when PSi doped in sol–gel and ormosil matrices. For instance, the absorption feature of PSi in silica matrix is dramatically changed with the emergence of two broad peaks, a peak centered at 258 nm and another broad feature at 350 nm. The presence of PSi in silica matrix affects the baseline of matrix when compared with the baseline of PSi in solutions as shown in Fig. 2ii. The peaks of PSi in the matrix increase with loss of baseline, which may be attributed to the interaction of particles and matrix. The changes in

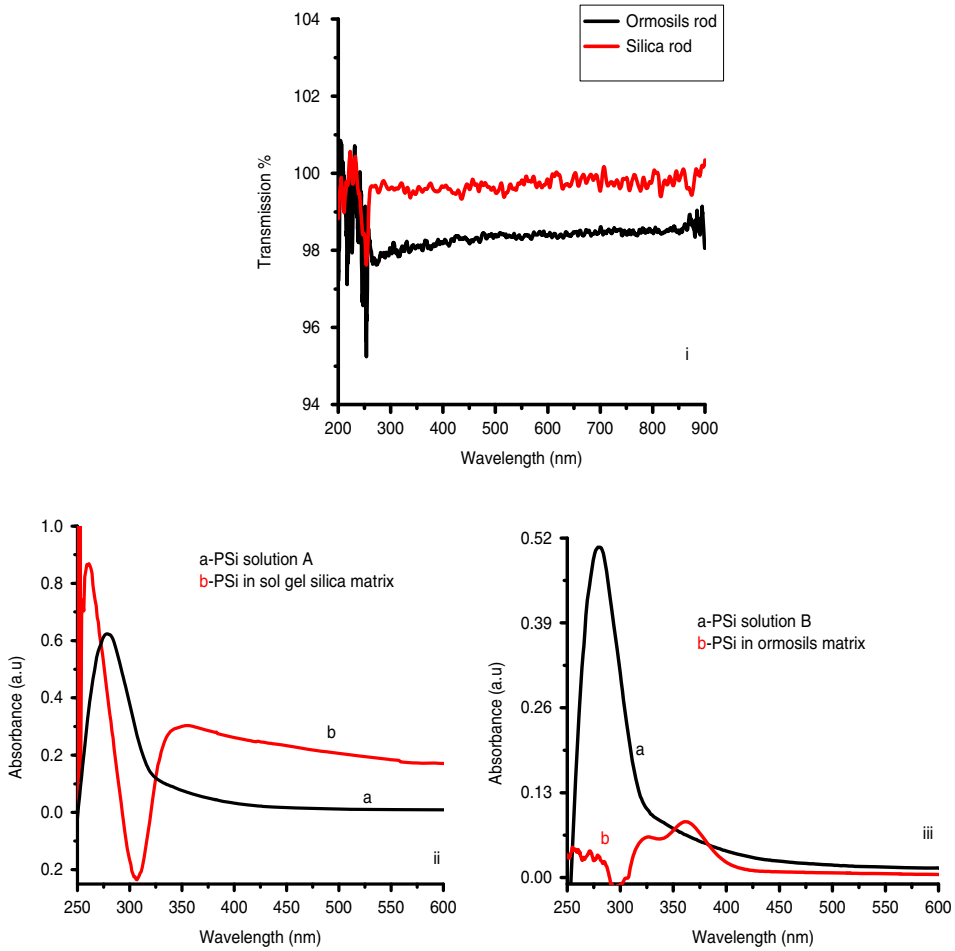

Fig. 2 **i** Transmission of UV–Vis spectra of silica and ormosil matrix, **ii** absorption spectra of porous Si-doped silica and **iii** ormosil host

absorption of PSi when doped in sol-gel matrix indicate the influence of matrix environment. The absorption feature of PSi in ormosils is observed with two peaks centered at 363 nm with a shoulder at 325 nm as shown in Fig. 2iii. Drastic change in the absorbance of PSi is observed in the ormosil matrix. The peaks are red-shifted, but no loss in baseline of composite ormosils is observed. The suppression in absorbance may correspond to the probability of change in densities for the PSi in ormosils. No significant reduction is observed in the volume of nanocomposite ormosil sol during the time of aging unlike the nanocomposite silica sol. Obviously, the intensity variation between the colloidal solution and PSi composites may be caused by the different proportion of PSi volume in matrices.

Though the PSi colloidal solutions were employed in silica matrices in previous work, the involvement of co-solvents [27–29] and DCCA [30] in the sol–gel process is different. In fact, the PSi solution used in [30] was dioxane but the number of rectangular wafer pieces taken was four in the preparation. The present PSi solution was synthesized using six rectangular wafer pieces in the same 20 ml volume of solvent, but there is clear difference in peak positions. Formamide was used as DCCA instead of DMSO and DMF since formamide can enable faster gelling, less stressing during gelling, etc. Formamide as DCCA is normally used to grow pores that are harder, larger and have more uniform pore size; these can help reduce cracking. DCCA as DMF can even produce larger pores after aging. Gels made with DMF do not crack at drying rates that sometimes destroy gels made with formamide or without any DCCA [39].

The comparison between the absorption feature of sol–gel silica and ormosils shows that the absorption property of PSi depends on the nature of matrix. A possible reason for the variation in absorption feature may be the matrix environment effect since the involvement of chemical composition in silica and ormosils plays an important role in matrix formation. Internal scattering of light within the silica and ormosil solid matrix is obviously different, which causes the absorbance of PSi because it reflects the sum of the scattering and absorption. In addition, the transition of sol to gel to solid phase during the aging process may influence the distribution of native PSi. However, a similar result was reported by Ramos et al. [40], that the confinement effects of Si nanoparticles in the oxide environment were reduced due to the presence of the SiO_2 matrix, which affects the absorption property. The shift in

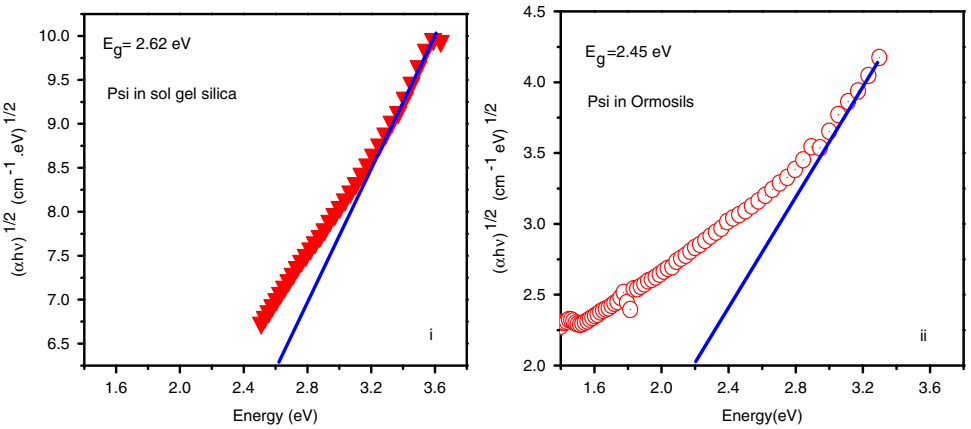

Fig. 3 Energy band gap (E_g) of PSi-doped **i** silica matrix and **ii** ormosils

peak positions may be attributed to the role of the interface between the PSi and matrices. A similar observation was reported by Daldosso et al. [16], that the interface of nc-Si/SiO_2 behaves differently with an extended transition region, which affects the optical properties. In the present case, the most possibility of this influence is from the interface of the SiO_2 matrix region since PSi is surrounded by SiO_2. Therefore, the same phenomenon can be observed clearly in Fig. 3, which shows the relationship between absorption coefficients as a function of photon energy. The absorption coefficient (α) can be calculated from the relation:

$$\alpha = \frac{A}{d}$$

where A is the absorbance of the samples and d is the thickness.

The optical band gap of the films is determined by applying the Tauc model [41] and the Davis and Mott model [42] in the high-absorbance region:

$$(\alpha h\nu) = C\left(h\nu - E_g\right)^n$$

where $h\nu$ is the photon energy, E_g is the optical band gap, C is a constant and n is a parameter that characterizes the optical absorption process, which is assumed theoretically to be equal to 1/2 and 2 for direct and indirect allowed transitions, respectively [43]. In order to find the band gap of samples, the relationship between $(\alpha h\nu)^{1/2}$ and $h\nu$ is plotted in Fig. 3i, ii. The value of band gap can be obtained by extrapolating the linear portion of the curve to the photon energy axis. As seen in Fig. 3, the value of band gap for PSi doped sol–gel silica and ormosils is different. It is assumed that different densities of nanoparticles in the matrix environment influence the absorption edges of PSi in the matrix. The band gap value for PSi composite sol–gel silica and ormosils is found to be a little different, but it is significant for the colloidal solutions. There is no major influence at the band gap of PSi by sol–gel compositions such as the co-solvent and DCCA. The band gap of PSi in silica prepared with THF as co-solvent and DMF as DCCA is not majorly different from that of dioxane and the formamide-based silica host. It means that the band gaps of PSi in solid media are not greatly influenced by the different compositions of matrices, but are found to be slightly influenced by the medium of matrix when compared between the solvents and the solid sol–gel matrix. The calculated band gaps of PSi composite silica [30] with the calculated absorption band gap of various PSi solutions have been reported by our group [31].

The SiO_2 matrix effect on the optical property of Si NCs was reported by the Gallas group [12]. Strong suppression in the optical property of Si NCs due to the dielectric functions of the SiO_2 matrix was observed by Ding et al. [13]. Another group [14] reported that the effect on the optical property of NCs was attributed to the influence on the arrangement of the Si NCs in the SiO_2 matrices by certain local-field effects. Moreover, a similar result obtained by Seinoa and his group [15] reported that small SiO_2 barriers lead to drastic changes in the optical properties of Si nanocrystals, such as the density of states, the dielectric function, and band-edge profiles.

3.2 Emission property

The emission spectra of PSi colloidal, composite silica, and ormosils were recorded using the 355 nm excitation wavelength and their comparison is displayed in Fig. 4i, ii. Encapsulation of PSi in the silica and ormosil matrix causes a change in the relative intensity. This effect is assumed due to the different proportion of PSi densities in matrices. The similar behavior of PSi in sol–gel silica prepared using different co-solvents and DCCA was observed in our previous reported work [29]. The emission peaks of PSi in the solvents were significantly shifted when included in sol–gel host. In fact, the emission property of PSi is influenced by the nature of sol–gel silica host, which usually depends on the co-solvent and DCCA used in the preparation [30]. For instance, the emission peaks of PSi in the sol–gel silica

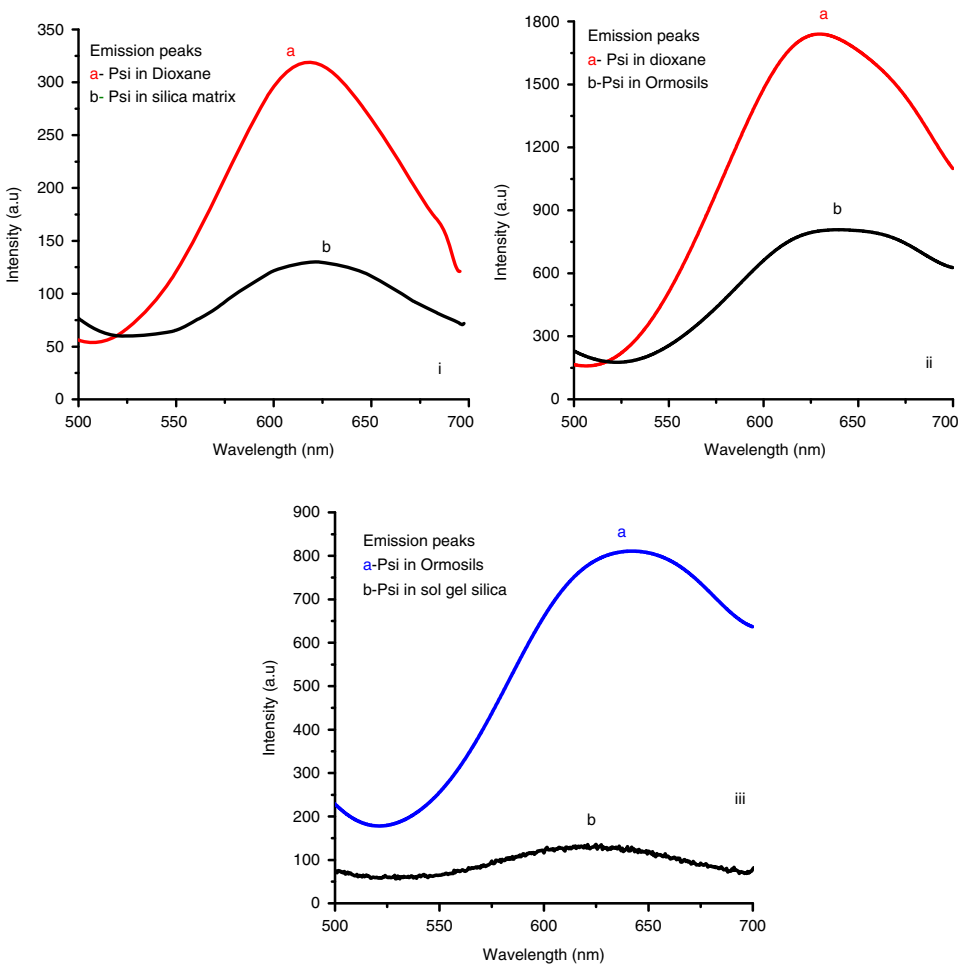

Fig. 4 Comparison emission spectra of PSi doped between **i** solution and silica, **ii** solution and ormisils and **iii** silica and ormosil matrix

prepared using THF and dioxane as co-solvent and DMF as DCCA are varied from the emission peaks of PSi in the silica host prepared using co-solvent of dioxane with DCCA as formamide. As clearly seen in Table 1, emission peaks of PSi in the formamide-based silica host appeared at 621 nm, whereas 605 and 593 nm are observed in the DMF-based silica host [29, 30]. Degradation in relative intensity of PSi in the silica hosts is observed from the emission intensity of colloidal solutions. There is clearly difference in the emission intensity of PSi in dioxane since both the solutions were prepared using equal quantity of wafer piece in the same volume of solvent. It is assumed that the number of optically active nanoparticles may differ in both the solutions. The higher optically active nanoparticles in solution may exhibit higher emission intensity. This may be a reason for the significant difference in emission intensity of PSi in dioxane observed between Fig. 4ii and i.

Reduction in emission intensity of PSi in the SiO_2 matrix can be caused by luminescence quenching. The reason for such effect in silica and ormosils may correspond to the result as reported by Liu et al. [44] that the emission line of NCs in SiO_2 sometimes may originate from defect states or interface states localized in the interface region between the silicon NCs and matrix. Further, they assumed that the emission of NCs should not be shifted with respect to annealing temperature if the emission originates from defect-related luminescence centers [44].

But the emission spectra of PSi composite silica and ormosil matrix originate from porous silicon because of the smaller crystalline sizes and as a result of quantum confinement within the nano size of the porous silicon. This characteristic of luminescence in PSi shows the crystallite band gap. Our results are in agreement with the one earlier reported by Fauchet and von Behren [45] proposed that the wide PL spectrum of electrochemical porous Si observed in the 550–750 nm region is due to exciton recombination in Si nanocrystals. Furthermore, there are several possibilities of such effects on the emission property of PSi in the matrices. The non-uniformity of PSi distribution in the matrix may also be attributed to slight change in emission intensity and peaks, since sol–gel-derived SiO_2 matrix is an oxygen environment that can have a substantial influence on luminescence property. In addition, the change of PSi native

Table 1 Comparison between the absorption and emission peaks of PSi in silica sol-gel and ormosils

Samples	Absorption peaks (nm)	Absorption peaks [29] (nm)	Absorption peaks [30] (nm)	Emission peaks (nm)	Emission peaks [29] (nm)	Emission peaks [30] (nm)
Silica sol–gel	258	260	269	621	605	593
	350	325	325			
Ormosils	325			639		
	363					

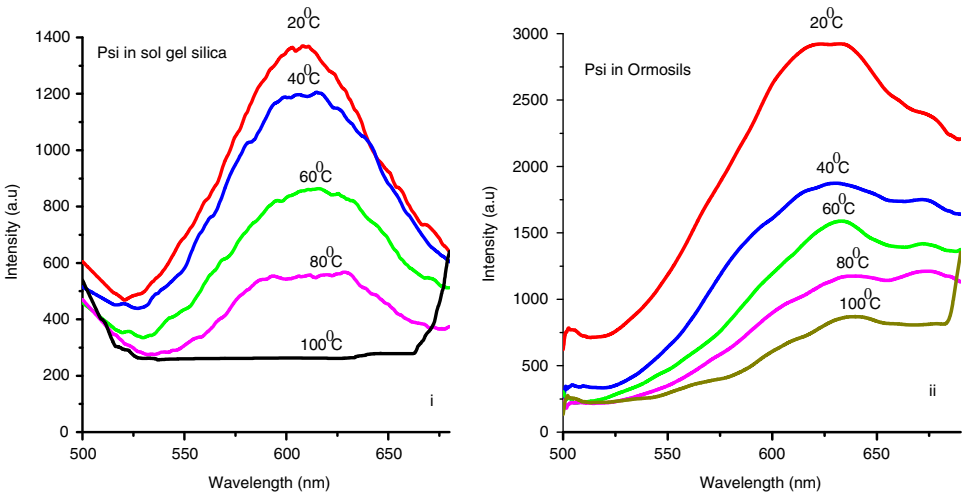

Fig. 5 Annealing effect on emission spectra of PSi-doped silica matrix and ormosils

in the sol–gel matrices during the evaporation of liquid (aging) normally influences the luminescence intensities. On the other hand, the emission intensity of PSi in ormosils is believed to be significantly strong as compared to the silica matrix. It is assumed that the rate of gelling of the ormosil matrix in order to solidify was faster due to polymerization with MMA, which can control the non-uniformity distribution of particles within the matrix. In general, ormosil matrix can be prepared and solidified in short time without any shrinkage of surface and with more uniformity. Therefore, the native of PSi within the ormosil matrix may reduce to influence with the distribution of particles. Though the degradation of emission intensity of PSi in ormosils is noticeable, it is clearly seen that emission of PSi in the ormosil matrix is much better than that in the silica matrix as shown in Fig. 4(i). Degradation in emission intensity of PSi in the presence of MMA was found: when polymers such as polymethylmethacrylate (PMMA) and polyvinyl pyrrolidone (PVP) were coated on the PSi surface, PL intensity of PSi was degraded. Further it was revealed that the addition of PMMA and PVP creates a PSi blunt and the shielded pores within the thin layer of polymers was observed, which caused a reduction in PL intensity [46]. Another group reported that addition of Si-ncs into conjugated polymer poly(methoxy-ethylexyloxy-p-phenylenevinilene) (MEH-PPV) leads to suppression of the PL band originating from surface states. Incorporation of Si-ncs in MEH-PPV polymer reduces the contribution of the PL band corresponding to surface states and defects [47]. In contrast, PL of polymer (PMMA)-PSi mixture-based film prepared by drop-casting on a glass slide was unaffected because the polymer protects the nanoparticles and prevents degradation of the PL [48].

In addition, previous studies reported by different groups [18–20] revealed that different synthesis techniques may affect the emission spectra of NCs in SiO_2 matrix, especially Si NCs in deposited SiO_2 films. But in the present case, PSi colloidal solutions are obtained by the same chemical etching technique and directly included in silica and ormosil sols at low temperature.

However, heating effect of the emission peaks of PSi within the environment of sol-gel-based silica and ormosil matrix was studied. We employed two PSi composite silica and ormosils sols. Two quartz cuvettes were heated up using a temperature controller attached to the sample chamber of a fluorescence spectrometer. In fact, the different PSi composite samples in the cuvettes were used to check the emission behavior under varied temperature. Obviously, PLs of different colloidal PSi solutions in silica or ormosils are observed since chemically synthesized porous silicon depends on the nature of solvent, etching magnitude of the surface and volume of hexachloroplatinic

(IV) acid (H_2PtCl_6) solution involved in etchant solution. Therefore, the PL property is influenced by these factors as reported in detail [31].

The annealing temperature of both the PSi samples was performed from 20–100 °C at an interval of 20 °C. The typical emission feature of PSi composite silica from 20 to 100 °C is shown in Fig. 5i. The dependence of the emission peaks and intensity on temperature was observed. The intensity of the PSi composites reduces with temperature increase till 80 °C and decline in the peak occurs at 100 °C. Bandwidth of the PSi spectrum becomes non-uniformi as the temperature increases. There is slight effect on peak position of PSi in both matrices with the temperature after 80 °C and the peak becomes broad. This might be the reason for the heat influence to change in the phase of matrix with interfacial SiO_2 matrix and PSi. The emission intensity of PSi in ormosil matrix decreases with a lesser influence of temperature when compared to composite silica matrix as shown in Fig. 5ii. The emission peak of PSi is still observed at 100 °C. This means that the emission of PSi in ormosils under annealing temperature can resist better than that in silica matrix. It may be possible that the structure of ormosils within an environment is quite rigid. One more reason to be considered is that silica sols evaporate faster during gelling, which may bring PSi distribution closer due to shrinkage of sol–gel structure.

Moreover, at annealing heat within sample chambers, the volume of Psi-doped silica sol inside cuvette is slowly reduced, but no significant decrease in volume of PSi ormosil sol is observed. This means that ormosil sol is more viscous and denser than the silica sol because the composition of ormosils involves monomers. We assume that the scattering/reflection or protection of photon light is possible when ormosil sol becomes viscous due to polymerization under heat treatment. Therefore, the relative PL values of PSi in ormosil sols is between 20–60 °C and falls down rapidly due to less number of photons passing through the sol medium. The PL values of composite silica sol slowly decay and evaporation of liquid is followed by rise in temperature.

Therefore, preparation of sol–gel based matrix involves H_2O and contains OH group in the matrix which can be affected upon heating with different temperatures. The decrease in emission intensity of dried sol–gel and ormosil sol may be related to this factor. In addition, we assume that PSi particles are surrounded by SiO_2 on the surface; when the temperature increases the size of PSi will be shielded by SiO_2 and may increase the size and induce loss in the emission due to scattering or reflection of photons from the matrix environment. A similar result obtained by Zhang et al. [21] interpreted that PL diminution in Si crystallites in silica sol–gel matrix was observed due to liberation of H_2O from the surface of silica sol–gel which contains a large number of OH groups. Further, reduction in the Si nanocrystallite PL was found most likely to be a result of oxidation and the thermal generation of nonradiative defects at the Si/SiO_2 interface. The decrease in the emission intensity of PSi composites matrix with heating can be correlated to the interpretation proposed by Posada group [23] that reduction of the density of optically active nc-Si particles in SiO_2 region is a result of chemical interactions and oxidation processes.

3.3 Spontaneous emission under picosecond laser source

The PSi composite rods were cut and the surface was polished before observation. The spontaneous emission (SE) of PSi composites and ormosil rods was studied using 355 nm laser source of the High-Power Picosecond Tunable Laser system. The exhibited SE from the composite samples can be seen in Fig. 6i and ii. The SE of PSi composite rods was examined by using a pumping energy of 4 and 8 mJ. When the pumped energy increases from 4 to 8 mJ, a significant change in spontaneous emission intensity is observed. This illustrates the dependence of emission intensity of PSi composite matrices on excitation intensity. This intensity of the nanocomposite samples is pronouncedly strong at 8 mJ. The PSi-doped ormosil rods yield a more noticeable change in intensity in comparison to the

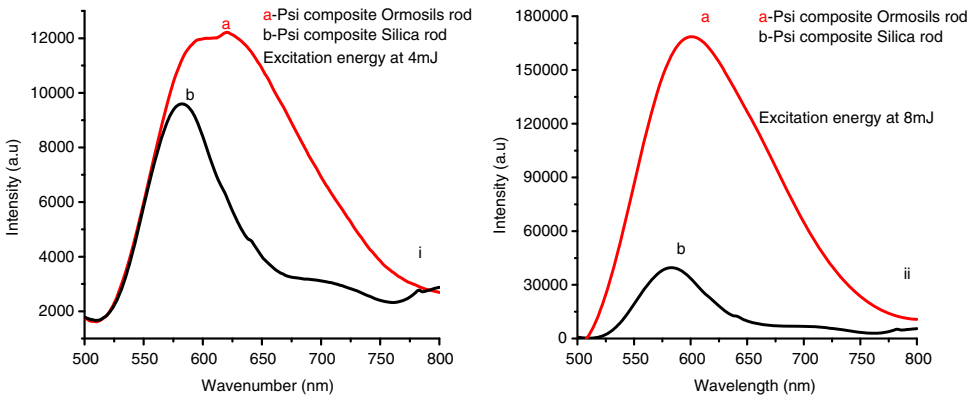

Fig. 6 Spontaneous emission spectra of PSi-doped **i** silica rod and **ii** ormosil rod at different pumping energy

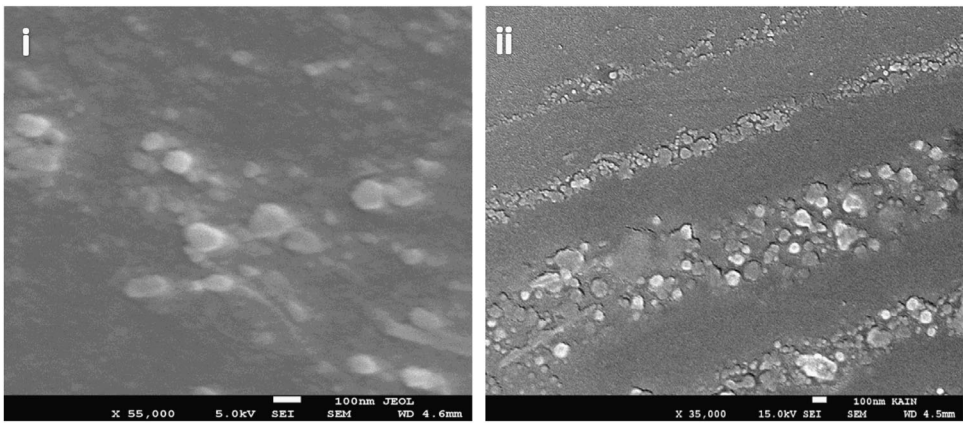

Fig. 7 FESEM images of PSi in **i** silica matrix and **ii** ormosils

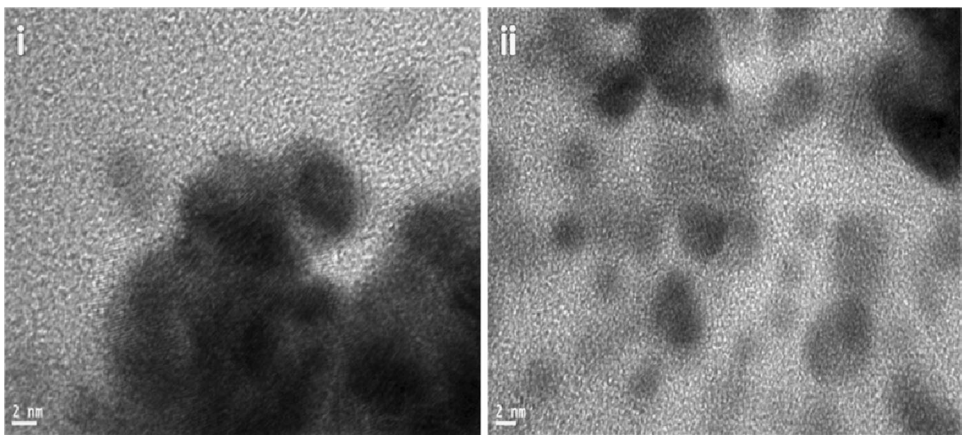

Fig. 8 TEM images of PSi particles in **i** silica matrix and **ii** ormosils

intensity of the PSi composite silica as seen in Fig. 4i, ii. It is seen that SE intensity of PSi composite ormosils is significantly inclined with higher excitation intensity, i.e., the increase is double, and is about 15 times greater than the excitation intensity at 4 mJ. The PSi composite silica rods exhibited three times stronger intensity with higher excitation intensities. This means a larger number of photons of PSi composite ormosils are excited by the pumped radiation over the composite silica type. No significant change in the band shape of the SE spectra of PSi in both matrices is observed with respect to excitation energy. But SE intensity for both PSi composite samples increases linearly with excitation intensity.

It is a matter of fact that enhancement of PL and spontaneous emission are greatly different since the SE was collected from the PSi composite rods whereas the emission (PL) spectra of PSi composite silica and ormosils were measured in quartz cuvettes. Moreover, power and excitation energy of picosecond laser source is much higher than the PL spectrometer. Therefore higher excitation energy can yield strong PL intensity due to more electrons in the excited state.

It may be worth mentioning that the SE peak of PSi in sol–gel silica shifts about 10 nm corresponding to the SE peak of ormosils. It may be attributed to the difference of interface between the PSi/silica matrix and PSi/ormosils because the interfacial region of sol–gel /ormosil matrix depends on the chemical composition involved in the sol-gel process. The weak SE intensity for the PSi composite sol–gel silica suggests that the phase and structure of silica matrix is glassy. Therefore, scattering of light may possibly be higher in the composite silica matrix than in the ormosils. An interesting point is that the emission peaks for both the PSi composite samples observed in spectrophotometer are strongly affected in position, intensity and band width in comparison with the peaks of SE produced by the laser source.

3.4 Surface morphology and particle sizes

The morphological structures of PSi in silica and ormosils were investigated by an FESEM. The presence of PSi particles in the surface of silica matrix and ormosils was observed. The surface structure with coverage of PSi is

closer in the silica matrix whereas Si particles in ormosils are nano-separated. The typical SEM images of PSi composite silica and ormosils are displayed in Fig. 7i and ii. PSi in the sol–gel silica and ormosil matrix have different structures. The silica surface seems to be aggregated within the surface of the SiO_2 environment. But the structure of PSi on the surface of ormosils is seen to be more regular. Both matrices have homogenous amorphous surfaces but the PSi in silica are sufficiently close to each other. The PSi native in silica is covered by the surface of the matrix. PSi particles are found to have a distinct structure on the surface of the ormosil matrix. It is believed that evaporation of H_2O during the gelling process can influence the structure of PSi in both types of matrix. Moreover, the silica-based sol–gel matrix shows faster transition from liquid (sol) to solid because of rapid liquid evaporation that leads to shrinkage of the matrix. Experimental observation suggests that initially the ormosil sol is denser and undergoes very less evaporation during drying due to polymerization process, which helps stabilize the PSi particles. It is possible that faster evaporation of liquid in sol-gel matrix can affect sol–gel condensation.

Figure 8 illustrates the typical TEM images taken by dropping the PSi composite sols onto a carbon-coated TEM grid at high resolution. The PSi particles in silica matrix are aggregated and have sizes of around 8 nm. While many of the particles are larger than 5 nm in diameter, the matrix also consists of some smaller size particles (below 5 nm).

Majority of PSi particles in the silica matrix are interconnected and distributed in the amorphous environment as shown in Fig. 8i. On the other hand, different sizes of PSi particles are found in the ormosil matrix, which are more or less 5–8 nm. PSi particles in the ormosils are well distributed and some of them are closer as shown in Fig. 8ii. It is confirmed that porous silicon particles are highly crystalline in nature at high resolution (not shown here). PSi particles present in the matrices are approximately spherical in shape. The highly crystalline nature and crystallographic plane of such PSi was also confirmed by diffraction image as reported in our previous work [31]. The difference in particle distribution in silica and ormosil matrix may be attributed to the effect of interface and the matrix environment.

4 Conclusions

Light-emitting porous silicon (PSi) fabricated by electroless chemical etching is studied in two types of sol–gel matrix. Direct encapsulation of the PSi colloidal solutions is performed. Crack-free composite rods based on PSi in silica and ormosils are successfully prepared. The present results reveal that the optical properties of PSi are influenced by the nature of the sol–gel matrix. Temperature dependence on the emission property of PSi in both composite matrices is observed. The structural variation of PSi in the matrix surface is revealed. Assuming the concentration of current colloidal solution is low based on weak absorbance, noticeable SE obtained from PSi composite rods is evident. The present study suggests that there is no major challenging problem regarding silicon nanoparticles in sol–gel-based matrices prepared at low temperature. There is no substantial loss of PSi emission in both types of matrix. Ormosil matrix is found to be superior based on its less influence on the PL property. Therefore, a highly dense and homogeneous size of PSi composite solid matrix may help to improve the emission intensity in future work. Further study on the mechanism of emission property in the composite matrix is under progress.

Acknowledgements The authors are thankful to the financial support of King Abdullah Institute for Nanotechnology, Deanship of Scientific Research, King Saud University, Riyadh, Saudi Arabia.

Compliance with ethical standards

Conflict of interest The authors declare that they have no competing interests.

References

1. Hayashi S, Yamamoto K (1996) Optical properties of Si-rich SiO_2 films in relation with embedded Si mesoscopic particles. J Lumin 70:352–363
2. Canham LT (1990) Silicon quantum wire array fabrication by electrochemical and chemical dissolution of wafers. Appl Phys Let 57:1046
3. Kim BS, Kim DI, Lee CW (2001) Photoluminescence from nano silicon materials prepared by photoelectrochemical methods. J Korean Phys Soc 38:245
4. Gosele U, Lehmann V (1995) Light-emitting porous silicon,. Mater Chem Phys 40:253–259
5. Chan WC, Nie S (1998) Quantum dot bioconjugates for ultrasensitive non-isotopicdetection. Science 281(5385):2016–2018
6. Bruchez M, Moronne Jr M, Gin P, Weiss S, Alivisatos AP (1998) Semiconductor nanocrystals as fluorescent biological labels. Science 281(5385):2013–2016
7. Michalet X, Pinaud FF, Bentolia LA et al. (2005) Quantum dots for live cells, in vivo imaging, and diagnostics. Science 307 (5709):538–544
8. Yerokhov VY, Melnyk II (1999) Porous silicon in solar cell structures: a review of achievements and modern directions for further use. Renew Sust Energ Rev 3:291–322
9. Arico AS, Bruce P, Scrosati B, Tarascon JM, Van Schalkwijk W (2005) Nanostructured materials for advanced energy conversion and storage devices. Nature Mater 4(5):366–377
10. Shin HC, Corno JA, Gole JL, Liu ML (2005) Porous silicon negative electrodes for rechargeable lithium batteries. J Power Sources 139:314–320
11. Parkhutic V (1999) Porous silicon—mechanisms of growth and applications. Solid State Electron 43:1121–1141

12. Gallas B, Stenger I, Kao CC, Fisson S, Vuye G, Rivory J (2005) Optical properties of Si nanocrystals embedded in SiO_2. Phys Rev B 72:155319
13. Ding L, Chen TP, Liu Y, Ng CY, Fung S (2005) Optical properties of silicon nanocrystals embedded in a SiO_2 matrix. Phys Rev B 72:125419
14. Ding L, Chen TP, Liu Y, Yang M, Wong JI, Liu YC, Trigg AD, Zhu FR, Tan MC, Fung S (2007) Influence of nanocrystal size on optical properties of Si nanocrystals embedded in SiO_2 synthesized by Si ion implantation. J Appl Phys 101:103525
15. Seinoa K, Bechstedta F, Kroll P (2012) Influence of separation of Si nanocrystals embedded in a SiO_2 matrix on electronic and optical properties. Mat Sci Eng B 177:1098–1102
16. Daldosso N, Luppi M, Ossicini S, Degoli E, Magri R, Dalba G, Fornasini P, Grisenti R, Rocca F, Pavesi L, Boninelli S, Priolo F, Spinella C, Iacona F (2003) Role of the interface region on the optoelectronic properties of silicon nanocrystals embedded in SiO_2. Phys Rev B 68:085327
17. Lalic N, Linnros J (1999) Light emitting diode structure basedon Si nanocrystals formed by implantation into thermal oxide. J Lumin 80:263–267
18. Shimizu IT, Hole DE, Townsend PD (1999) Light emission from ion beam induced silicon nanoclusters in silicon dioxide: role of cluster-cluster interactions via a thin oxide. Nucl Instrum Methods Phys ResB 148:980–985
19. Kanzawa Y, Kageyama T, Takeoka S, Fujii M, Hayashi S, Yamamoto K (1997) Size-dependent near-infrared photoluminescence spectra of Si nanocrystals embedded in SiO_2 matrices. Solid State Commun 102:533–537
20. Kahler U, Hofmeister H (2001) Visible light emission from Si silicon nanocrystalline composites via reactive evaporation of SiO. Opt Mater 17:83–86
21. Zhang L, Coffer JL, Zerda TW (1998) Properties of luminescent Si nanoparticles in sol-gel matrices. J Solgel Sci Technol 11:267–272
22. Svrcek V, Pelant I, Rehspringer JL, Gilliot P, Ohlmann D, Cregut O, Honerlage B, Chvojka T, Valenta J, Dian J (2002) Photoluminescence properties of sol–gel derived SiO layers doped with porous silicon. Mater Sci Eng C 19:233–236
23. Posada Y, Miguel LS, Resto O, Weisz SZ, Kim CH, Shinar J (2004) Optical properties of nanocrystalline silicon within silica gelmonoliths. J Appl Phys 96:2240–2243
24. Karlash AY, Zakharko YE, Skryshevsky VA, Tsiganova AI, Kuznetsov GV (2010) Photoluminescence properties of silica aerogel/porous silicon nanocomposites. J Phys D: Appl Phys 43:335405
25. Amonkosolpan J, Wolverson D, Goller B, Polisski S, Kovalev D, Rollings M, Grogan MD, Birks TA (2012) Porous silicon nanocrystals in a silica aerogel matrix. Nanoscale Res Lett 7:397
26. Borsella E, Falconieri M, Botti S, Martelli S, Bignoli F, Costa L, Grandi S, Sangaletti L, Allieri B, Depero L (2001) Optical and morphological characterization of Si nanocrystals/silica composites prepared by sol–gel processing. Mat Sci Eng B 79:55–62
27. Khan MN, Al Dwayyan AS, Al Salhi MS, Al Hoshan M (2012) Study on characteristics of silicon nanocrystals within sol-gel host. J Expt Nanosci 7(2):120–132
28. Khan MN, Al Dwayyan AS (2012) Influence on structural and PL property of nanocrystals silicon doped sol gel matrix. J Optoelectron Adv M 14(5):448–454
29. Al Dwayyan AS, Khan MN, Al Salhi MS (2012) Optical characterization of chemically etched nanoporous silicon embedded in sol gel matrix. J Nanomater (7) Article ID:713203
30. Khan MN, Al Dwayyan AS, Al Hossain MS (2013) Morphology and optical properties of a porous silicon-doped sol-gel host. Electron Mater Lett 9(5):697–703
31. Khan MN, Khan MMA, Al Dwayyan AS, Puzon LJ (2014) Comparative study on electronic, emission, spontaneous property of porous silicon in different solvents. J Nanomater (14): Article ID:682571
32. Li HR, Zhang HJ, Lin J, Wang SB, Yang KY (2000) Preparation and luminescence properties of ormosil material doped with $Eu(TTA)_3$phen complex. J Non-Cryst Solids 278:218–222
33. Akcakir O, Therrien J, Belomoin G, Barry N, Muller JD, Gratton E, Nayfeh M (2000) Detection of luminescent single ultrasmall silicon nanoparticles using fluctuation correlation spectroscopy. Appl Phys Lett 76:1857–1859
34. Nayfeh M, Akcakir O, Therrien J, Yamani Z, Barry N, Yu W, Gratton E (1999) Highly nonlinear photoluminescence threshold in porous silicon. Appl Phys Lett 75:4112–4114
35. Sarathy J, Shih S, Jung K, Jung K, Tsai C, Li KH, Kwong DL, Campbell JC, Yau SL, Bard AJ (1992) Demonstration of photoluminescence in nonanodized silicon. Appl Phys Lett 60 (13):1532–1534
36. Shih S, Jung KH, Hsieh TY, Sarathy J, Campbell JC, Kwong DL (1992) Photoluminescence and formation mechanism of chemically etched silicon. Appl Phys Lett 60(15):1863–1865
37. Khan MN, Al Dwayyan AS (1998) Influence of solvent on the physical and lasing properties of dye-doped sol–gel host. J Lumin 128(2008):1767–1770
38. Wright JD, Nico AJM (2001) Sommerdijk sol-gel materials, chemistry and applications Gordon and breach. Science Publishers, Amsterdam.
39. Jeffrey C and Scherer GW (1990) 'Sol gel science, the physics and chemistry of sol gel Processing by Academic Press, San Diego.
40. Ramos LE, Furthmuller J, Bechstedt F (2004) Effect of backbond oxidation on silicon nanocrystallites. Phys Rev B 70:033311
41. Tauc J, Grigorovic R, Vancu A (1966) Optical properties and electronic structure of amorphous germanium. Phys Status Solidi B 15(2):627–637
42. Davis EA, Mott NF (1970) Conduction in non-crystalline systemsV. Conductivity, optical absorption and photoconductivity in amorphous semiconductors. Philos Mag 22:903–922
43. Fukutani K, Kanbe M, Futako W, Kaplan B, Kamiya T, Fortmann CM, Shimizu I (1998) Band gap tuning of a-Si:H from 1.55 eV to 2.10 eV by intentionally promoting structural relaxation. J Non Cryst Solids 227–230:63–67
44. Liu X, Zhang J, Yan Z, Ma S, Wang Y (2001) Photoluminescence from SiC nanocrystals embedded in SiO_2. Mater Phys Mech 4:85–88
45. Fauchet PM, vonBehren J (1997) The strong visible luminescence in porous silicon: quantum confinement, not oxide-related defects. Phys Status Solidi (b) 204(1):R7–R8
46. Kulathuraan K, Pandiarajan J, Prithivikumaran N, Jeyakumara N, Natarajan B (2012) Structural and Optical Properties of Polymer Composites/Porous Silicon. AIP Conference Proceedings 1451: 215
47. Vladimir S, Hiroyuki F, Michio K (2009) Luminescent properties of doped free standing silicon nanocrystals embedded in MEH-PPV. Sol Energ Mat Sol Cells 93:774–778
48. Kirkey WD, Cartwright AN, Li X, He Y, Swihart MT, Sahoo Y, Prasad PN (2004) Optical properties of polymer-embedded silicon nanoparticles. Mat Res Soc Symp Proc 789(30):1. N15